

氏 名	くさま ともえ
授 与 学 位	博士 (工学)
学 位 授 与 年 月 日	平成28年3月25日
学位授与の根拠法規	学位規則第4条第1項
研究科, 専攻の名称	東北大学大学院工学研究科 (博士課程), 金属フロンティア工学専攻
学 位 論 文 題 目	Cu-Al-Mn 合金におけるサイクル熱処理誘起異常粒成長
指 導 教 員	東北大学教授 貝沼 亮介
論 文 審 査 委 員	主査 東北大学教授 貝沼 亮介 東北大学教授 粉川 博之 東北大学教授 古原 忠 東北大学准教授 大森 俊洋

論文内容要約

Chapter 1: Introduction

The most practically utilized superelastic (SE) alloy at present is the intermetallic compound NiTi, called Nitinol, due to its good SE properties. However, its practical application is limited to small size parts due to high material cost and low cold-workability. On the other hand, on account of its higher cold-workability, lower material cost and the same level of SE property in comparison with Nitinol, the Cu-Al-Mn alloy is attracting much attention as a possible SE material for large-scale components such as seismic dampers and isolators.

In Cu-Al-Mn based alloys, it is known that the maximum SE strain dramatically increases with increasing relative grain size, d/D or d/w (d : average grain diameter, D : diameter of wire, w : width of plate) [1, 2]. Therefore, a large grain size is required to realize an excellent SE property in large samples. Cyclic heat treatment (CHT) between the β single-phase and the $\alpha + \beta$ two-phase region, as shown in the phase diagram of Fig. 1[3], is known to be effective to obtain a microstructure with a large grain size. Actually, an extremely coarse grain size of several centimeters has been reported by using CHT.

There are only a limited number of previous reports on abnormal grain growth (AGG) induced by CHT, and details of the mechanism of this grain coarsening are still unknown. In this thesis, the mechanism of AGG induced by CHT is examined and

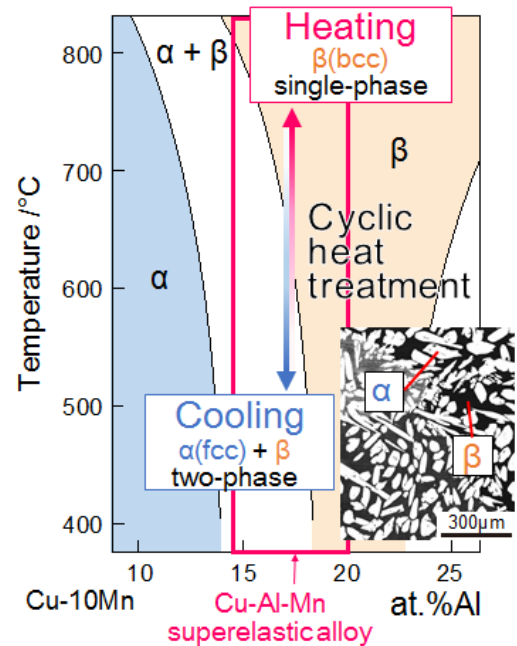


Fig. 1 Cu-Al-10at.%Mn vertical section diagram[3] and cyclic heat treatment.

the CHT conditions appropriate to obtain larger grains are proposed.

This thesis is composed of 6 chapters.

Chapter 2: Abnormal grain growth and cyclic heat treatment

In this chapter, to extract the factors important to obtain AGG by CHT, the relationship between each condition in CHT and final grain size is investigated.

It is revealed that the conditions especially related to the cooling process, such as cooling rate and final cooling temperature, strongly affects the grain size after heat treatment. By orientation analysis with electron back-scatter diffraction (EBSD) patterns for the specimens subjected to solution heat treatment followed by cooling to the two-phase region, it was confirmed that precipitation of the α phase results in formation of a subgrain microstructure (SGM) in the β matrix phase and that the misfit angles among the subgrains increase with decreasing cooling temperature. Then, even after subjecting solution heat treatment again, the SGM remains in the β phase, while the α phase is perfectly dissolved, as shown in Fig. 2. Moreover, whereas existing entirely in all the grains in the normal grain growth (NGG) condition, the SGM is only partially observed in the grains in the AGG condition. This suggests that the grain boundaries of the abnormal grains migrate, sweeping out the SGM, and that the AGG phenomenon is related to the SGM.

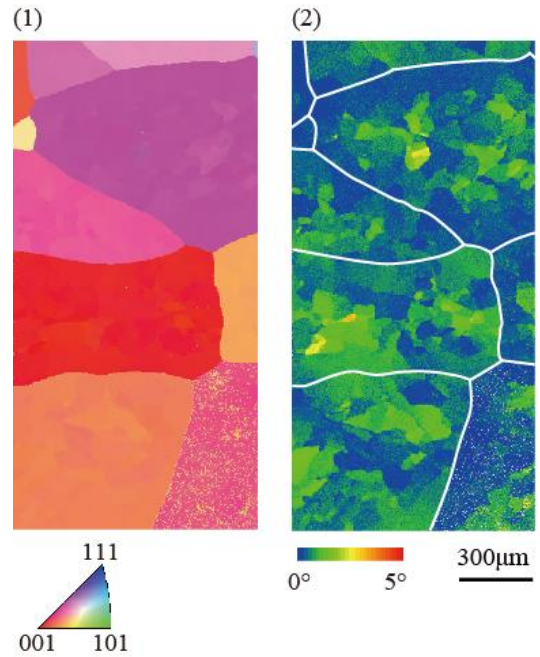


Fig. 2 The subgrain microstructure in the β matrix in Cu-17Al-11.4Mn (at.%) alloy. (1) Inverse pole figure mapping. (2) Grain reference orientation deviation mapping. White lines show grain boundaries.

Chapter 3: Normal and abnormal grain growth behaviors and the origin of abnormal grain growth

In this chapter, the NGG and AGG behaviors are reported in comparison each other, and for the AGG, the effects of multi-cycle in the CHT are also presented.

The time dependence of the mean grain diameter is generally given by $d^n - d_0^n = kt$, where d_0 , n and k are the initial mean diameter, the grain growth exponent and constant, respectively. It was clarified that in the NGG at 800 °C and 900 °C, the grain growth exponent is estimated to be about $n = 6.5$, which is larger than those in many other metallic alloys. This retardation behavior may result from the pinning effect by impurity particles and/or the grooving effect by surface roughness. Actually, the grain growth in specimens with a smooth polished surface becomes slightly faster than that with an unpolished surface.

For the examination of AGG in specimens with an SGM, two types of specimens with different SGM were prepared: one is a sample with the SGM obtained by one-time cyclic heat treatment (1CHT), which is the same as that reported in chapter 2, and the other is that obtained by five-times cyclic heat treatment (5CHT),

where the solution heat treatment temperature in each CHT is fixed slightly higher than the $\alpha+\beta$ two-phase region to prevent the occurrence of the AGG. It is confirmed that the SGM obtained by 5CHT shows larger misorientation in the sub-boundaries and possesses higher boundary energy. The boundary migration rates of AGG in specimens finally-annealed at 850 °C are shown in Fig. 3. The migration rate in the 5CHT sample is 2.3 - 5.5 times larger than that in the 1CHT sample. This result can be explained as being due to the difference in the sub-boundary energy estimated from the misorientation of the sub-boundaries. This suggests that the sub-boundary energy of the SGM is the dominant driving forces in the AGG.

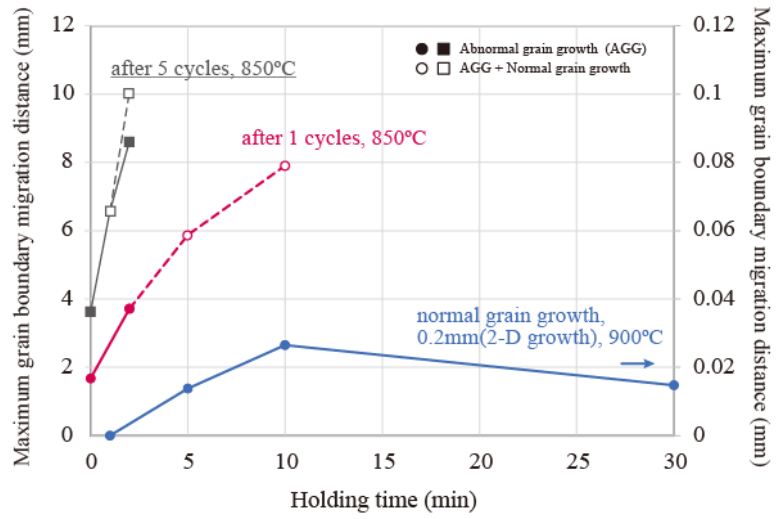


Fig. 3 The grain boundary migration distance of AGG at 800 °C and 850 °C in specimens with different sub-boundary misorientation, compared with that of NGG at 900 °C.

Chapter 4: Origin of subgrain microstructure in the cooling process

In this chapter, to understand the formation mechanism of the SGM in the β matrix in the cooling process, results of microstructural observation and analysis for specimens with the $\alpha + \beta$ two-phase are presented.

The mean subgrain size after heating up to the β single-phase region is almost proportional to the mean size of the α precipitates, which depends on the cooling condition. Furthermore, it was observed that in the early stage in the formation of SGM, a sub-boundary domain expanded from the α/β phase boundary to the β matrix region. Here, the α/β phase boundary observed in the specimen cooled to 600 °C was semicoherent and the orientation relationship (OR) was Bain OR, K-S (Kurdjumov-Sachs) OR or Pitsch OR. In diffusional phase transformation, it is known that the semicoherent phase boundary growing with the ledge-wise growth process has two different kinds of dislocations, i.e., sessile and glissile interfacial dislocations, to release strain introduced by the change of crystal structure, where the sessile misfit dislocation migrates only by climbing, while the glissile relaxation dislocation can migrate by gliding [4, 5]. It is considered that the glissile dislocations glide out from the phase boundary to the β matrix region and form dislocation networks, i.e., sub-boundaries, in the β matrix during growth of the α phase.

Chapter 5: Formation of colossal grains utilizing abnormal grain growth

In this chapter, the CHT for AGG most effective to obtain colossal grains is optimized using the information revealed in chapters 2 - 4.

Migration rate, v , of grain boundary is generally given by $v = M \cdot \Delta G$ with boundary mobility, M , and driving force, ΔG . The first approach for increasing v is by the increase of driving force for AGG, which can be

realized by heightened misorientation of sub-boundaries due to many CHTs, as mentioned in Chapter 3 and/or by decreasing subgrain size due to the introduction of smaller α precipitates, as mentioned in Chapter 4. In the small subgrain size, however, AGG simultaneously occurs in many grains, and the final average grain size does not become large. As for using the mobility of the grain boundary, it was found that a textured microstructure formed before CHT is effective to improve the AGG due to the reduction of the fraction of grain boundaries with high mobility.

By subjecting the newly designed CHT, huge single-crystal Cu-Al-Mn alloy bars with a diameter of $\phi 16$ mm and a length of about 400 mm were fabricated from normal polycrystalline samples, as shown in Fig. 4. The bars were also confirmed to show excellent SE properties.

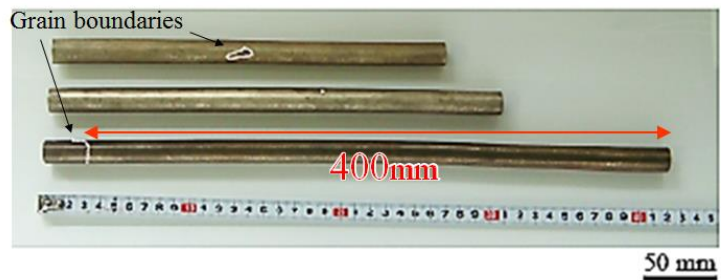


Fig. 4 Huge grains in a Cu-Al-Mn alloy bar with a diameter of $\phi 16$ mm obtained by appropriate cyclic heat treatment.

Chapter 6: Conclusions

In this chapter, the contents of chapters 1 through 5 are summarized.

Acknowledgements

This work was supported by Grant-in-Aid for JSPS Fellows (Grant Number 26•7381) from the Japan Society for the Promotion of Science (JSPS).

References

- [1] Y. Sutou: Doctor's Thesis, Tohoku University, (2000).
- [2] Y. Sutou, T. Omori, R. Kainuma and K. Ishida: *Acta Mater.*, **61** (2013) 3842-3850.
- [3] R. Kainuma, S. Satoh, X. J. Lin, I. Ohnuma and K. Ishida: *J. Alloys Comp.*, **266** (1998) 191-200.
- [4] H. I. Aaronson, T. Furuhashi, J. M. Rigsbee, W. T. Reynolds, Jr. and J. M. Howe: *Metall. Trans. A*, **21A** (1990) 2369-2409.
- [5] T. Furuhashi, K. Wada and T. Maki: *Metall. Mater. Trans. A*, **26A** (1995) 1971-1978.